

Constraints on Additional Satellites of Pluto from HST Images

Eliot F. Young

*Southwest Research Institute, Department of Space Studies, 1050 Walnut St, Boulder CO
80302*

`efy@boulder.swri.edu`

and

Marc W. Buie

Lowell Observatory, 1400 W. Mars Hill Rd., Flagstaff, AZ 86001

ABSTRACT

We describe a search for satellites of Pluto from HST images obtained in 2002 and 2003 with the High Resolution Camera (HRC). We have processed these images with PIXON reconstruction software. The post-processed frames show no satellites interior to Charon's orbit down to a 5σ limit of $B=25.1$ at 4 Pluto radii. The B-magnitude limit degrades to $B=22.8$ at $1 R_P$. No satellites are found outside of Charon's orbit down to a 5σ limit of $B=25.9$. This data set covers a radius of $12.5''$, about 670 times smaller than Pluto's Hill sphere radius. Over a dozen asteroids were serendipitously detected in the 12 HST visits.

Subject headings: Pluto; Satellites: general; Image processing

1. Introduction

There are many reasons to search for additional satellites within the Pluto-Charon system. The origin of the Pluto-Charon pair is thought to be the result of a giant impact (Canup 2005). If Charon formed close to Pluto's Roche limit (around $2.5 R_P$) and subsequently evolved outward to its present distance of $16 R_P$, then the region inside of Charon's orbit should be swept clean. However, an outer satellite may have been trapped in a resonance with the migrating Charon and moved outwards in step with Charon.

The Hubble Space Telescope (HST) program GO-9391 was designed to map Pluto’s albedo distribution in V- and B-filters. This high-resolution data set is well suited to probe the space between Pluto and Charon for faint objects. In addition, about 0.15% of Pluto’s Hill sphere is covered by the HST exposures, out to a radius of about 550 thousand kilometers.

Over a dozen asteroids were serendipitously detected in the HST frames, but no Pluto satellites were detected, either inside or outside of Charon’s orbit. The rest of this paper discusses our efforts to sharpen the HST images and lower the detection threshold.

2. Observations

The HST program GO-9391 includes 384 images of Pluto and Charon taken over twelve visits from June 2002 through May 2003. Each visit consists of 32 dithered images, 16 taken in the F555W filter and 16 in the F435W filter. These filters are close analogs to the Johnson V- and B-filters, respectively. All images were taken with the Advanced Camera for Surveys (ACS) High Resolution Camera (HRC). The nominal platescale for the HRC is $0.025''$ per pixel. At this resolution, Pluto subtends 4 pixels and Charon subtends slightly more than two. The Pluto-Charon separation of $19,636 \pm 8$ km (Tholen and Buie 1997) is never more than 40 pixels at this platescale.

The $0.025''$ platescale subsamples the point spread functions (PSFs) at both wavelengths. Figure 1 shows PSFs generated with TinyTim v6.3 software (Krist and Hook 2005). Figure 1 also illustrates the major side-effect of the HRC being an off-axis array, that a square on the sky plane maps onto a trapezoid on the CCD. (The PSF diffraction spikes, for example, are perpendicular on the sky plane but skewed in each HRC image.)

These images were processed with most of the standard STScI on-the-fly pipeline steps, including bias and dark current subtraction and flat field normalization, but not multi-drizzle or cosmic ray removal. Both of those pipeline steps will modify some of the pixel values for moving (solar system) targets. The typical sky noise in the resulting F435W and F555W frames is 4 to 6 DN (data numbers). Aperture photometry around Pluto yields total counts from 97,000 to 147,000 in the F435W filter, depending on Pluto’s rotational phase (Pluto’s lightcurve amplitude was been measured at 30% for the orientation it presented in the early 1990s (Buie et al. 1997). Counts from Charon in the F435W filter are close to 20,000 DN.

PIXON reconstruction (or some other form of PSF fitting or deconvolution) is necessary to examine the regions near Pluto and Charon. Figure 2 shows raw and reconstructed pairs of images. Without reconstruction, the PSF halos around Pluto and Charon contaminate pixels between the two objects at levels 20 to 500 times higher than the clear-sky noise level.

The full HRC array is 1024 x 1024 pixels, but the GO-9391 subframes were half-size (1024 x 512 pixels) to reduce the read-out time. Each exposure samples roughly a 25.6'' x 12.8'' region of space approximately centered on Pluto. The orientation of this rectangle on the sky plane changed from visit to visit as a function of the HST’s roll orientation, so a 25'' x 25'' region around Pluto is sampled over the course of several months. In section 4 we examine whether a satellite could escape detection by temporally avoiding the long axis of the HRC rectangle.

3. Results

3.1. Brief Description of the PIXON Reconstruction Procedure

The PIXON reconstruction technique deconvolves an observation given an estimate of the PSF (Puetter and Yahil 1999). The PIXON algorithm decomposes an observation into a set of centrally peaked kernels of varying widths. Two principles govern how PIXON chooses a set of pixel kernels to represent the reconstructed image. First, the residuals between the model and the data must be small compared to the noise on a pixel-by-pixel basis. The model is the convolution of the PIXON solution with the PSF. All comparisons take place in data space. Second, PIXON seeks the smoothest, least informative set of kernels that is consistent with the residuals constraint. This “minimum information” constraint keeps spurious artifacts out of the solution unless significant residuals would result from their omission.

In practice, the PIXON algorithm depends critically on the estimated noise and, to a lesser extent, the accuracy of the PSF. If the noise estimate is too high, the PIXON reconstruction will be too simple and smooth. Actual image features will be ignored, since they fall below the erroneous noise threshold. If the noise estimate is too low, then bright noise outliers will be interpreted as astronomical sources, since they are higher than the too-low noise estimates.

We estimate the noise at each pixel as the quadratic sum of the “sky noise” and the Poisson source noise. The sky noise is a combination of read noise, dark current noise and background noise. We use the DAOPHOT routine “SKY.PRO” (part of the IDL astron library) to estimate the sky noise. The source noise is assumed to have a Poisson distribution, i.e., the square root of data counts (in electrons).

$$\sigma_{pixel} = \frac{\sqrt{(\sigma_{sky}g)^2 + Dg}}{g} \quad (1)$$

where σ_{sky} is the sky noise returned by “SKY.PRO” (in DN, or data numbers), D is the absolute value of the pixel signal (in DN), and g is the gain (in electrons per DN). The HST pipeline has already multiplied pixel values by the gain (originally 2 electrons per DN), as documented by the FITS keyword “BUNIT” having a value of “ELECTRONS.”

PIXON provides feedback regarding the quality of the fit in the form of χ^2 , the standard weighted sum of squared residuals, and Q , the difference between the actual χ^2 minus the expected value of χ^2 (a function of the number of degrees of freedom), normalized by the expected value of χ^2 . The Q parameter should be close to one. If Q never reaches unity (and the PSF is reasonably accurate), the noise estimates are probably lower than the actual noise. If Q reaches values less than unity in a single iteration, then the noise estimates are too high and PIXON easily finds a solution that is uselessly smooth.

3.2. Registration and Median Filtering

There are many sources and cosmic ray hits in each individual HRC frame. Fortunately, the parallax of the Pluto-Charon system is large enough that distant sources (stars or galaxies) move by tens of pixels between consecutive exposures. A simple median filter applied to a stack of 3 or more exposures removes nearly all of the background sources and cosmic ray hits. Any satellite of Pluto, including grazing satellites, will move by less than a pixel relative to Pluto over an eight-exposure period (about 10 minutes).

We coregister the frames before applying a median filter. Each dither sequence within a visit consists of 16 separate exposures. We subsample the exposures by a factor of ten (using the IDL routine “REBIN.PRO”), then cross-correlate the first frame with each of the subsequent 15 frames. The 15 subsampled exposures are shifted by integral pixels in the subsampled grid to align their cross-correlation peaks, then the shifted frames are resampled to their original resolution.

Pluto and Charon (and potential satellites of Pluto) are not removed by the median filter since they appear over the same pixels in each frame. Charon’s motion with respect to Pluto is never more than 0.6 pixels per hour (when Charon’s velocity vector lies completely within the sky plane). At a duty cycle of 86 seconds per exposure (12 second integrations plus 74 seconds for overheads), Charon’s motion is barely detectable over a 16-frame dither sequence. Interior satellites can move faster – a grazing satellite would move up to 2.4 pixels per hour. We don’t want potential satellites to move by more than a pixel in the plutocentric reference frame. For this reason we split each 16-frame dither sequence into two 8-frame stacks, each spanning about ten minutes (0.4 pixels for a grazing satellite). We

compare results from the two stacks to help eliminate false positives.

It is possible that a highly eccentric satellite would be moving very quickly at perihelion. The limiting velocity is the escape velocity at Pluto’s surface, which is 1.41 times higher than the velocity of a grazing satellite. Even this extreme case would only move 0.6 pixels in a ten-minute period, so we are confident that a median-filtered stack of 8 consecutive coregistered images will not filter out any Plutocentric objects in the field.

Besides filtering stars and cosmic ray hits, a median-filtered stack has lower noise per pixel than an individual frame, by \sqrt{N} for a stack of N frames. This significantly improves our detection threshold - a median-filtered stack of 8 frames has a typical measured sky noise of 0.97 to 1.15 DN, compared to about 4.0 DN in single frames. This improvement amounts to lowering the detection threshold by over a magnitude. In the calculations that follow, we will conservatively estimate the 5σ sky noise to be 6.0 DN for a stack of eight 12-sec exposures.

3.3. Results from PIXON-Processed, Median-Filtered, Coregistered Stacks

A look at the PSFs generated by TinyTim shows that a point source will have Strehl ratios of 0.21 in the F435W filter and 0.16 in the F555W filter. The goal of PIXON processing is to take all of the light in the distributed PSF and put it back into a single pixel (for point sources). PIXON (and other PSF-fitting strategies) can significantly improve the detection threshold. For example, an object whose peak pixel is 1σ above the noise could be a 5σ detection if PIXON successfully restores the distributed 80% of the object’s signal into its peak pixel.

In practice, the computer-generated TinyTim PSFs are not exactly accurate. Both PIXON and Lucy-Richardson deconvolution of our HRC images with TinyTim PSFs produce solutions with artifacts at the first Airy ring.

The F435W images produced cleaner solutions than the F555W ones, and we only use the 192 F435W images to search for satellites around Pluto. All of the PIXON-processed images exhibited some artifacts where the first Airy ring intersects the diffraction spikes, but the magnitude of the problem varies considerably from stack to stack. Note that the Airy ring artifacts are actually quite small, less than one percent of counts on a Pluto pixel, but they still potentially obscure faint objects near Pluto. In section 3.4 we obtain cleaner results in Pluto’s immediate vicinity by PIXON-processing individual F435W exposures in the original (non-rectangular) HRC coordinates.

Figure 3 shows that no sources associated with the Pluto-Charon system are found at the 5σ level. We can determine the limiting magnitude by converting DN to magnitudes. The HST FITS keyword “PHOTFLAM” is provided for flux calibration purposes; it specifies the flux (in $\text{ergs sec}^{-1} \text{\AA}^{-1}$) per DN for each exposure. For the F435W images, PHOTFLAM is typically $5.45 \times 10^{-19} \text{ ergs sec}^{-1} \text{\AA}^{-1}$. The flux from a $B=0$ magnitude object is $6.61 \times 10^{-9} \text{ ergs sec}^{-1} \text{\AA}^{-1}$ (Zombeck 1992). The F435W exposure times are 12 seconds, so the magnitude equivalent to a single DN is 27.9, as given by (2).

$$B_{DN} = -2.5 \log_{10} \left(\frac{5.45 \times 10^{-19}/12}{6.61 \times 10^{-9}} \right) = 27.9 \quad (2)$$

The magnitude equivalent to the 5σ noise level of 6.0 DN for a 12-sec exposure is 25.9.

$$B_{5\sigma} = -2.5 \log_{10} \left(\frac{6 \times 5.45 \times 10^{-19}/12}{6.61 \times 10^{-9}} \right) = 25.9 \quad (3)$$

How big an object corresponds to $B=25.9$ at 30 AU? Aperture photometry of Charon in the F435W images typically yields around 20,000 DN, or 3,333 times the 5σ counts of 6 DN. For objects with the same albedo as Charon, the limiting radius is 57.7 times smaller than Charon’s radius of 621 km (Young and Binzel 1994), or 10.75 km.

3.4. Results from PIXON-Processed Single Exposures

It is likely that a stack of 8 exposures, even carefully coregistered exposures, are slightly smeared compared to individual exposures. We have run the PIXON algorithm on all 192 of the F435W exposures in the original (skewed) HRC coordinate system. 192 distinct TinyTim PSFs are required, since the PSF in the skewed HRC coordinate system is position dependent. These PIXON results are only applicable to Pluto’s local neighborhood, but our goal is to clean up the first Airy ring around Pluto, out to about 6 pixels from Pluto’s surface.

Figure 2 compares a raw and PIXON-processed frame in the HRC coordinates. Although we are not sure why the PSF does a better job in some cases than others, it probably has to do with very small displacements of elements in the HRC optical train. For example, we have fit the PSF focus position as a free parameter for every exposure as part of our ongoing work to map Pluto’s surface albedo distribution. We find that the focus parameter varies monotonically over the course of an orbit (presumably as function of time in or out of sunlight). We have used these focus positions in the TinyTim input files to generate more

accurate PSFs.

In any case, there are several PIXON reconstructions where there are no artifacts outside of a radius of $2 R_p$. Unfortunately, the limiting magnitudes in this case are not as low as in the coregistered stack case, both because the stacks have lower noise than single frames and also because of the stray light in the neighborhood of Pluto produces noise levels several times higher than over the open sky.

For single exposures, the Poisson source noise is equivalent to the sky noise when the source counts are 16 DN. When counts are 50, 100 or 500 DN (typically at 6, 4, and 2 pixels from Pluto’s surface), the 5σ noise levels are 40.6, 53.9, and 113.6 DN, respectively. The equivalent B magnitudes are 23.9, 23.6, and 22.8, which translate to radii of 28.0, 32.3, and 46.8 km, assuming Charon-like albedos.

For most of the projected region within one arcsecond (40 pixels) of Pluto, the median-filtered 8-frame stacks provide lower detection limits and smaller size constraints than the single-exposure PIXON-processed frames. Are the single exposures helpful at all? Yes – within the the first Airy ring surrounding Pluto (in the F435W filter, the first Airy ring is about 6–7 pixels, or $3.5R_p$, beyond Pluto’s surface). The best of the PIXON-processed 8-frame stacks all have significant artifacts at the first Airy ring at about the 50 DN level. In contrast, the cleanest of the PIXON-processed single frames have signals of 3 DN or less at the first Airy ring.

4. Discussion

A search for Pluto’s satellites is more interesting in the context of where satellites are favored or prohibited. Stern et al. (1994) investigated dynamical boundaries on stable regions in the vicinity of Charon’s orbit. They point out that Pluto’s Roche limit at $2.5 R_p$ is likely to be a inner boundary for additional satellites. They seeded the Pluto-Charon system with 1700 massless test particles with initial semi-major axes between 0.15 – 3.0 times a_C (Charon’s semi-major axis) and integrated their orbits for 1000 Charon-periods ($T_C = 6.387$ days). The stability of a region was evaluated on the basis of the surviving fraction of test particles, where “survival” means that a particle did not enter the Roche boundary of Pluto or the Hill sphere of Charon.

Stern et al. (1994) find that test particles with semimajor axes between $\sim 0.47 T_C$ and $\sim 2 T_C$ are unstable on timescales of a thousand orbit periods, with a sharp inner edge at $0.47 T_C$ but some narrow zones of relative stability around $1.8 T_C$. It appears that the 5:2 and 3:1 Charon resonances are unstable zones. In addition, any Charon co-orbitals are expected to

be unstable, since the Charon-Pluto mass ratio of 0.122 ± 0.008 (Olkin et al. 2003) is larger than the stability limit ($\mu_2 = \frac{m_2}{m_1+m_2} \leq \sim 0.0385$) for stable horseshoe or tadpole orbits (e.g., Eq. 3.145 of Murray and Dermott (1999)).

Of course, the fact that an orbit is forbidden does not preclude us from looking hard at those regions. Furthermore, the latest published eccentricity for Charon’s orbit is 0.0076 (Tholen and Buie 1997), which suggests that a third body may be present in the Pluto-Charon system. Tholen and Buie (1997) note that roughly half of Charon’s putative eccentricity may be due to unknown center-of-light vs. center-of-mass offsets. Even so, an eccentricity of 0.003 is problematic. Stern et al. (2003) examine close encounters and impacts with other Kuiper belt objects as possible sources for Charon’s eccentricity and find that explanation very unlikely.

If Charon did indeed form close to Pluto from post-collisional accretion fragments and evolved outwards, one would expect outer satellites to be trapped in Charon resonances and pushed outward as Charon evolved to its present semimajor axis of $\sim 16 R_p$. Our observations provide contiguous coverage of a $12.5''$ region around Pluto and better than 50% coverage of a $25''$ region. A $6.25''$ radius corresponds to circular-orbit period of $15.6 T_C$, while the $12.5''$ radius corresponds to $44.2 T_C$. This region outside of $2.4 T_C$ is the preferred region for Pluto satellite candidates, yet we find no satellites brighter than a 5σ limit of $B=25.9$.

The completeness of our search between radii of $6.25''$ and $12.5''$ is determined by the HST roll angles. Figure 4 shows that the roll angles (the “ORIENTAT” FITS keyword) vary slightly for observations that were obtained over a span of a few days. In other words, a significant fraction of the region between $6.25''$ and $12.5''$ is not covered by these observations. Notice that the last five visits span 50 days and nearly a 90° sweep of roll angles. A satellite with a semimajor axis of 122,500 km (corresponding to $6.25''$ at greatest elongation) will have a Plutocentric period of 100 days, and a semimajor axis of twice that (corresponding to $12.5''$ at greatest elongation) translates to a period of 282 days. The 50-day span of the last five GO-9391 visits is short enough to ensure that any satellite located between $6.25''$ to $12.5''$ from Pluto would be sampled by the last five visits.

The $B=25.9$ magnitude limit corresponds to a radius of 10.75 km for an object with a Charon-like B-filter albedo of 0.4. A fainter object could be larger – a 0.04 albedo object would have $10\times$ the surface area or a radius of 34.0 km.

Pluto’s approximate Hill sphere radius is given by

$$R_H = a_{PL} \left(\frac{m_{PL}}{3m_{Sun}} \right)^{1/3} = 0.051 AU \quad (4)$$

where $a_{PL} = 39.44$ AU, $m_{PL} = 0.0022$ Earth masses, and $m_{Sun} = 3.33 \times 10^5$ Earth masses. At Pluto’s distance of 30 AU, a radius of 0.051 AU subtends $352''$. Our images subtend a relatively minute $6.25''$ in one dimension and $12.5''$ in the other. Our sampled area is a little less than one thousandth of the projected area of Pluto’s Hill sphere. Obviously, our limited sampling area does not rule out the possibility of more distant satellites of Pluto.

The detections of serendipitous asteroids provides a somewhat independent estimate of the detection limit. Figure 5 shows observations from one HST visit in which 8 asteroids appear in the Pluto-centered exposures. The brightest of these asteroids has Pluto-centric relative motions of -0.020 pixels per second in the y-axis and -0.0093 pixels per second in the x-axis. When we coregister (and median-filter) a stack of 8 frames to this bright asteroid, we find that eight asteroids are clearly visible. The faintest of these asteroids has counts of 26.7 DN (in a 5×5 aperture), equivalent to a B-magnitude of 24.3.

5. Conclusions

We have examined stacks of B-filter exposures to look for satellites of Pluto. For several of these stacks, TinyTim v6.3 PSFs are sufficient to deconvolve the rectified HRC images and look for faint satellites. For the regions exterior to Charon’s orbit out to $12.5''$, we can rule out satellites brighter than $B=25.9$ at the 5σ level, which is equivalent to 6 electrons.

Noise levels are higher in between Pluto and Charon due to the scattered counts from Pluto and Charon. Typical contour radii around Pluto for 50, 25 and 12.5 DN levels are 8, 9, and 10 pixels, respectively. The 8-pixel radius is the outer radius of the Airy ring in the F435W filter. Outside of that radius we get better detection limits from the coregistered, PIXON-processed, median-filtered stacks of 8 consecutive frames. For an 8-frame stack, the 50-DN contour (9-pixel radius) 5σ level is 12.6 electrons (equivalent to a B-magnitude of 25.1). At the 10-pixel radius, the 5σ level is 6.7 electrons, equivalent to $B=25.8$.

Within the 8-pixel radius ($4 R_P$), we use single PIXON-processed frames to set the detection limit, since the 8-frame stacks produced artifacts after PIXON processing. The detection limits from single frames range from $B=22.8$ within the first $1 R_P$ above Pluto’s surface to $B=23.9$ at $3 R_P$ from Pluto’s surface.

Based on observations made with the NASA/ESA Hubble Space Telescope, obtained at the Space Telescope Science Institute, which is operated by the Association of Universities for Research in Astronomy, Inc., under NASA contract NAS5-26555. These observations are associated with program #GO-9391.

Support for program #GO-9391 was provided by NASA through a grant from the Space Telescope Science Institute, which is operated by the Association of Universities for Research in Astronomy, Inc., under NASA contract NAS5-26555

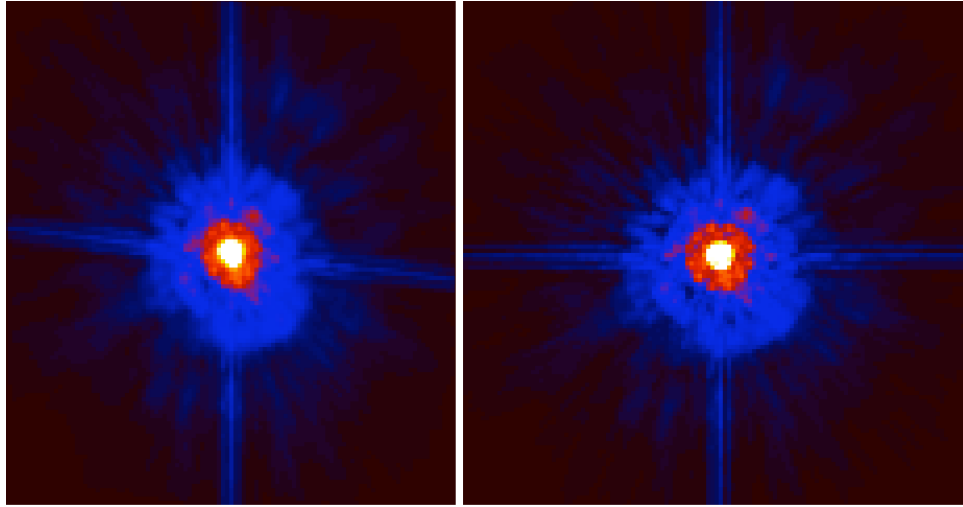
We are grateful to Bill Ward and David Nesvorny for helpful discussions.

Facilities: HST.

REFERENCES

- Buie, M. W., Tholen, D. J., & Wasserman, L. H. 1997. Separate Lightcurves of Pluto and Charon. *Icarus*, 125, 233
- Canup, R. M. 2005. A Giant Impact Origin of Pluto-Charon. *Science*, 307, 546
- Krist, J. & Hook, R. 2004. The Tiny Tim Users Guide version 6.3. <http://www.stsci.edu/software/tinytim>.
- Murray, C. D., & Dermott, S. F. 2000, *Solar System Dynamics*, by C.D. Murray and S.F. Dermott. ISBN 0521575974. <http://www.cambridge.org/us/catalogue/catalogue.asp?isbn=0521575974>. Cambridge, UK: Cambridge University Press, 2000.
- Olkin, C. B., Wasserman, L. H., & Franz, O. G. 2003. The mass ratio of Charon to Pluto from Hubble Space Telescope astrometry with the fine guidance sensors. *Icarus*, 164, 254
- Puetter, R. C., & Yahil, A. 1999. The Pixon Method of Image Reconstruction. ASP Conf. Ser. 172: Astronomical Data Analysis Software and Systems VIII, 172, 307
- Stern, S. A., Parker, J. W., Duncan, M. J., Snowdall, J. C. J., & Levison, H. F. 1994. Dynamical and observational constraints on satellites in the inner Pluto-Charon system. *Icarus*, 108, 234
- Stern, S. A., Bottke, W. F., & Levison, H. F. 2003. Regarding the Putative Eccentricity of Charon’s Orbit. *AJ*, 125, 902
- Tholen, D. J., & Buie, M. W. 1997. The Orbit of Charon. *Icarus*, 125, 245
- Young, E. F., & Binzel, R. P. 1994. A new determination of radii and limb parameters for Pluto and Charon from mutual event lightcurves. *Icarus*, 108, 219

Zombeck, M. V. 1990. Handbook of space astronomy and astrophysics. Cambridge University Press, 1990, 2nd ed.



Eliot Young-Pluto Satellites-FIG 1

Fig. 1.— A model point spread function for the F435W filter on the center of the HRC detector generated with TinyTim v6.3. The PSF on the right has undergone a transformation to rectify the skewed HRC coordinate system. The PSF on the left represents a point source as it would appear in an unprocessed HRC frame. These PSFs have been normalized to unity. The peak pixel value is 0.21.

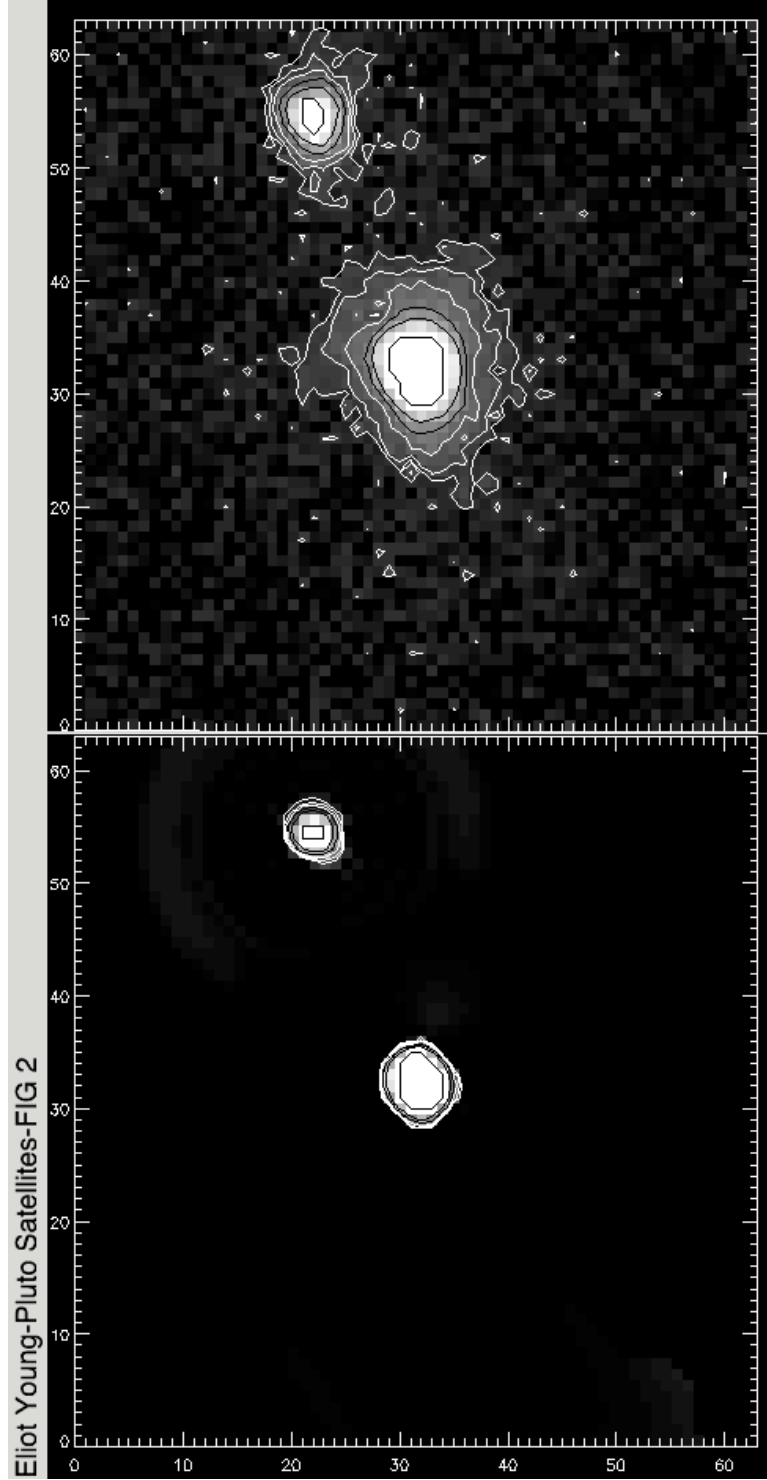


Fig. 2.— A raw (top) and PIXON-processed frame. Both frames have identical grayscale stretches ranging from 0 to 50 DN. The lower panel is one of the better PIXON results – the small smudge above Pluto and the arcs around Charon are only 2.6 DN at their peak levels, less than half of the 5σ level (6 DN). The contour levels are 12.5, 25, 50, 100, 200 and 500 DN. As the oblique shapes of Pluto and Charon indicate, this exposure is in HRC coordinates, not undistorted coordinates

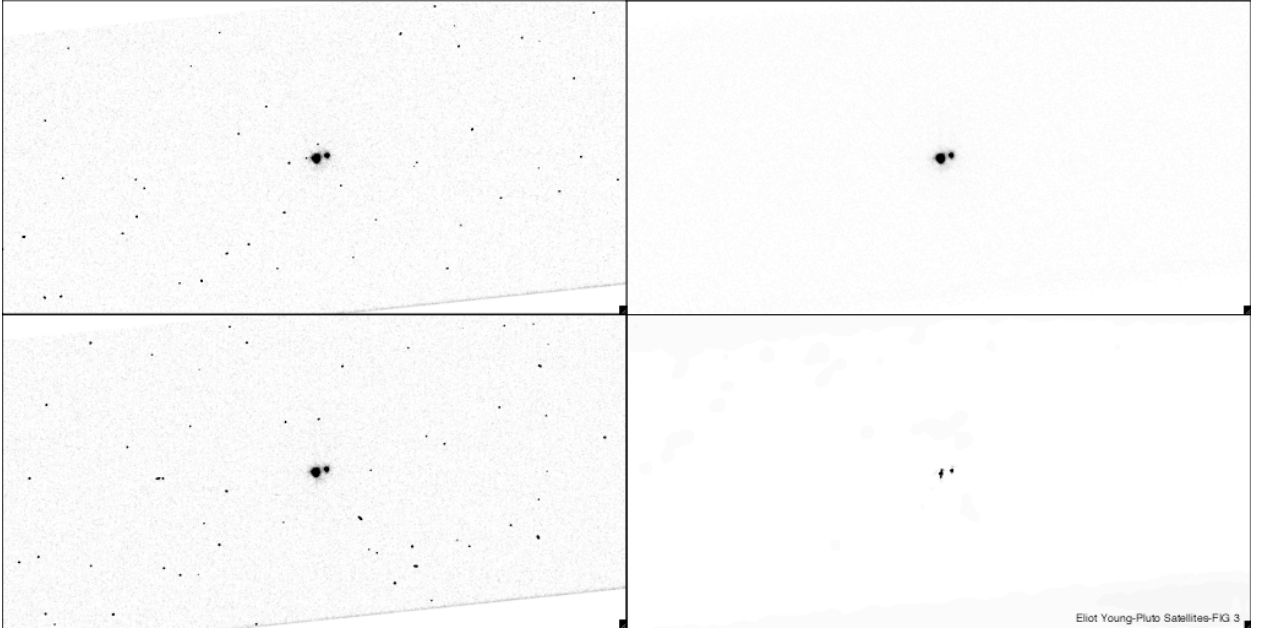
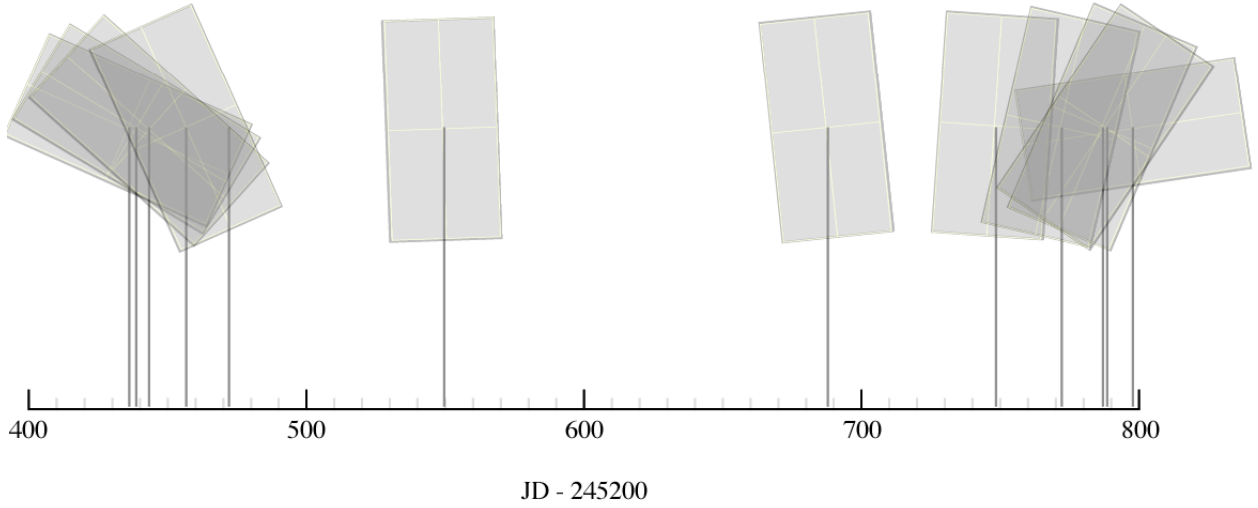


Fig. 3.— Two consecutive HRC frames (undistorted) on the left side show Pluto, Charon, and many stars and cosmic rays. After median-filtering a stack of 8 coregistered frames (upper right), the stars and cosmic rays are filtered out. Any object associated with the Pluto-Charon system would show up in the median-filtered stack. The median-filtered stacks were PIXON-processed with a TinyTim-generated PSF (e.g., lower right) to increase the sensitivity to faint sources, but no satellites were found. The minimum and maximum display values for all four panels range from 0 to 6.0 DN, the 5σ level. The Airy ring artifacts show up around Pluto and Charon in the PIXON-processed plot, but no satellites are visible at the 5σ level.



Eliot Young-Pluto Satellites-FIG 4

Fig. 4.— A timeline of HRC observations displaying the orientation of the HRC field. The long axis spans $25''$, the short axis spans $12.5''$. Equatorial north is “up” in this plot, and the field orientations are given by the “ORIENTAT” keyword in the FITS file header. To catch 100% of satellites brighter than $B=25.9$ between $6.25''$ and $12.5''$, the roll angle would have to vary by 90° on a timescale shorter than 100 days, the period of a satellite at $6.25''$ from Pluto – which it nearly does.



Fig. 5.— A superposition of 4 HRC images (j8fb06ltq, j8fb06m1q, j8fb06m6q, and j8fb06maq), each separated by about 5 minutes. The four frames have been rectified and centered on Pluto to within a tenth of a pixel. At least eight asteroid trails are visible in this stack of exposures, the faintest of which has a B -magnitude of about 24.3.